

A Low-Cost Optical Sensor for Non contact Vibration Measurements

*Original*

A Low-Cost Optical Sensor for Non contact Vibration Measurements / Perrone, G., Vallan, A.. - In: IEEE TRANSACTIONS ON INSTRUMENTATION AND MEASUREMENT. - ISSN 0018-9456. - STAMPA. - 58:5(2009), pp. 1650-1656. [10.1109/TIM.2008.2009144]

*Availability:*

This version is available at: 11583/1994504 since:

*Publisher:*

IEEE-INST ELECTRICAL ELECTRONICS ENGINEERS

*Published*

DOI:10.1109/TIM.2008.2009144

*Terms of use:*

This article is made available under terms and conditions as specified in the corresponding bibliographic description in the repository

*Publisher copyright*

(Article begins on next page)

© 2009 IEEE. Personal use of this material is permitted. Permission from IEEE must be obtained for all other uses, in any current or future media, including reprinting/republishing this material for advertising or promotional purposes, creating new collective works, for resale or redistribution to servers or lists, or reuse of any copyrighted component of this work in other works.

**A Low Cost Optical Sensor for Non Contact Vibration Measurements**

G. Perrone and A. Vallan

Published in: Instrumentation and Measurement, IEEE Transactions on (Volume:58 , Issue: 5 )

Date of Publication: May 2009

Page(s): 1650 - 1656

ISSN : 0018-9456

INSPEC Accession Number: 10560705

Digital Object Identifier : 10.1109/TIM.2008.2009144

Sponsored by : IEEE Instrumentation and Measurement Society

# A Low Cost Optical Sensor for Non Contact Vibration Measurements

G. Perrone, *Member, IEEE*, A. Vallan

**Abstract**—This paper presents a new non-contact method to measure vibrations using a low cost optical approach, yet able to provide sub-micrometer resolution. The transducer exploits a simple optical setup based on an intensity detection scheme implemented with plastic optical fibers, while innovative non-demanding spectral data processing allows compensating for the vibrating surface reflectivity and the gains of the measurement chain. The performance of the proposed system have been assessed, through the comparison with other techniques, performing several measurement tests using targets vibrating at frequencies from few hertz up to several tens of kilohertz and with different values of reflectivity.

**Index Terms**— *Optical Fibers, POF, Optical Sensors, Vibration measurements, Vibrometers.*

## I. INTRODUCTION

THE problem of measuring vibrations is a very important topic that encompasses different areas of civil and industrial engineering. Some vibrations are intentional and necessary for the proper functioning of devices (e.g. shakers, ultrasonic cleaning baths, rock drills, etc.) while others are just unwanted effects due to manufacturing tolerances or to the response of the structure to external stresses. Therefore a large number of methods to measure the frequency and/or the amplitude of the vibration using mechanical, electrical or optical devices has been proposed in the literature [1], [2]. However, regardless of the working principle, these approaches can be subdivided into two broad categories depending on the necessity of physical contact with the vibrating object or not. Generally, contact sensors, such as strain gauges and piezoelectric accelerometers, are less expensive but can be used only for bulky vibrating objects in order to minimize their influence on the measurement, although the progress in micro/nano-machining is continuously reducing the size constraint that makes the sensor perturbation negligible. For example, MEMS-based accelerometers are emerging as very popular and cheap devices suitable also for consumer applications. However, despite their excellent characteristics, in many cases of practical interest contact sensors cannot be used either because of the difficulty of reaching the vibrating object or for its extremely small size. Profiling the deformation of ultrasonic transducers or - more generally - measuring the vibration in localized tiny spot, up to several tens of kilohertz, with micrometer displacements, are typical examples where contact sensors are not effective. Optics provides excellent technologies to overcome

these limitations allowing the development of high performance non-contact sensors, namely the most interesting since they truly do not perturb the vibrations. Many optical approaches have been proposed in the literature, the most popular being the interferometric method and the laser Doppler vibrometer (LDV). In interferometric methods, a laser signal beam is directed onto a moving target and the back-reflected light is recombined with part of the incident light, using different schemes (e.g. Michelson or Mach-Zendher schemes) [2]. Interferometers are characterized by very high performances in terms of resolution and bandwidth but are also very expensive and impose stringent mechanical requirements because the alignment is critical. Laser vibrometers exploit the Doppler effect [3] to measure the frequency of a vibration; the amplitude is then recovered by integration of the velocity, and thus it may result not accurate enough for the precise measurement of very small displacements. Typically, a Helium-Neon or Argon ion laser with a power of 10 mW to 20 W is used to obtain high signal-to-noise ratios, and this may pose some limitations in the general usage, given the safety requirements. LDV can be used to measure both translational or torsional vibrations and are characterized by very high frequency response, but the accuracy is highly dependent on alignment between emitted and reflected beams. However the main limitation to their wide spreading comes from their cost: although some laser vibrometers are commercially available as portable device, they are still quite expensive. Moreover they are very sensitive to environmental conditions such as variations of temperature or fluctuations in the air flow between the instrument and the target as can occur in industrial applications. Alternative, cheaper, optical solutions using glass fiber bundles have been proposed [5]; in this case some of the fibers in the bundle illuminate the target and some other fibers collect the back-reflected light and the amplitude of vibration is recovered from the measurement of the intensity modulated back-reflected light. This approach can give very good results but, being based on amplitude variations, it is sensitive also to the reflectivity of the vibrating surface and to the gains of the measurement chain. The compensation for the surface reflectivity, has been addressed in [6] using several receiving fibers, but it requires a proper calibration of the sensor.

An alternative method is proposed in this paper where we present a high resolution and cheap optical sensor to measure vibrations up to several tens of kilohertz, using an intensity detection scheme followed by an innovative non-demanding data processing to compensate for the vibrating surface reflectivity and measurement chain gains. The setup is based on the detection of a modulated non-

coherent beam light (LED), delivered to and from the analyzed surface by plastic optical fibers (POF). POF permit the realization of a remote sensing head without the complications and costs of glass fibers thanks to their superior light collecting capability that translates into an overall ease of handling. POF have typically a 0.98 mm core (thus much larger than the  $9\ \mu\text{m}$  core of glass single mode fibers used for high performance optical communications and the  $62.5\ \mu\text{m}$  core of multimode glass fibers) made of Poly-Methyl-Methacrylate (PMMA) surrounded by a thin (about  $20\ \mu\text{m}$ ) fluorinated polymer cladding. The large core size together with the high numerical aperture (about 0.5) account for a series of advantages of POF over glass fibers and most notably easier connectorization, less attention to tolerances with a subsequent reduction in the connector requirements and costs, possibility to use low cost transceivers based on LED instead of laser diodes, enhanced flexibility to shock and vibration thanks to a lower Young's modulus, etc. POF exhibit also some disadvantages such as much larger attenuation and dispersion, but these drawbacks are of negligible impact for the sensing applications, and specifically for those addressed in this paper.

The remaining of the paper is organized as follows: in Sect. II we describe the working principle of the developed sensing system and in Sect. III we present the technique proposed to compensate for the variations in the surface reflectivity. Then in Sect. IV we analyze the sensitivity and uncertainty of the sensing system and in Sect. V we present the assessment of the performances through some experimental results achieved in different working conditions. Finally in Sect. VI we draw the conclusions.

## II. THE SENSOR WORKING PRINCIPLE

The sensing head is made by two plastic optical fibers arranged as shown in Fig. 1; one fiber is used to transmit the non coherent light from a LED driven by a transconductance amplifier, while the other fiber collects the light reflected by the target whose vibrations  $s(t)$  have to be measured. The target distance from the fiber tips is  $d$ . An alternative and further miniaturized sensing head uses the same fiber both to deliver and collect the light beams, with the addition of a coupler to separate these two signals. At the receiver side a photodiode PD connected to a transimpedance amplifier is used to convert the light into an electric signal  $v_R(t)$  that may be written as:

$$v_R(t) = A \cdot v_L(t) \cdot \frac{P_r(d)}{P_t} \quad (1)$$

where  $v_L(t)$  is the voltage applied to the LED driver,  $P_r(d)/P_t$  is the ratio between the optical powers at the receiver and at the transmitting fiber surfaces, and the term  $A$  takes into account all the factors independent from  $d$ , such as the amplifier gains, the fiber and connector losses, the photodiode responsivity and the target reflectivity.

The target vibrations modify the distance between the

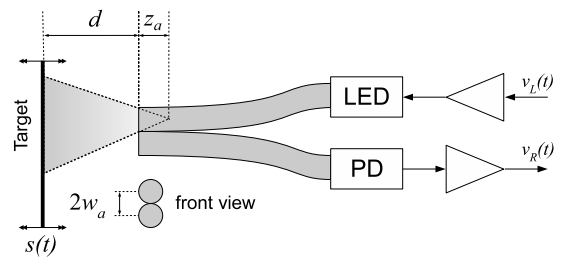


Fig. 1. Sketch of the sensor layout.

fiber tips and the target itself and, therefore, the received optical power  $P_r(d)$ . The exact relationship between the target position and the received power depends on fiber characteristics, such as the numerical aperture, the core radius, the fiber surface polishing and on the target surface. In the case of a reflective surface and a gaussian beam, the received optical power can be analytically obtained as a function of the target distance  $d$ , of the fiber radius  $w_a$  and of the position of the light asymptotic cone vertex  $z_a$  as [4]:

$$\frac{P_r(d)}{P_t} = \frac{2}{\zeta^2} e^{-8/\zeta^2} \quad (2)$$

where  $\zeta = 1 + 2d/z_a$ . Fig. 2 shows an example of the typical measured behavior of the power ratio versus the distance; the maximum of the received optical power is for  $\zeta = \sqrt{8}$  that is for:

$$d_{MAX} = \frac{\sqrt{8} - 1}{2} z_a \quad (3)$$

The power increases monotonically for normalized distance lower than  $d_{MAX}$ ; then at larger distances reduces approximately like  $1/d^2$ , as expected from theoretical considerations. Although the value of  $z_a$  could be computed from the a priori knowledge of all the parameters affecting the received power versus distance relationship, it is more practical to determine it from a measurement of this curve, given the difficulty to quantitatively evaluate some of these parameters such as the surface quality, the polishing angle of the fiber tip, etc. Considering a standard POF, the maximum received power is for a target distance close to about 1.6 mm so that  $z_a \cong 1.75$  mm.

Target displacements  $s(t)$  due to vibrations behave like small changes of the target distance from the fiber tips  $d(t) = d_0 + s(t)$ , where  $d_0$  is the mean value of the target distance. Therefore the ratio  $P_r/P_t$  can be locally approximated around  $d_0$  as (straight dotted line in Fig. 2):

$$\frac{P_r(d)}{P_t} \simeq R_0 + R_1 \cdot (d - d_0) \quad (4)$$

that can be rewritten as:

$$\frac{P_r(t)}{P_t} \simeq R_0 + R_1 \cdot s(t) \quad (5)$$

and the detected signal can be expressed as:

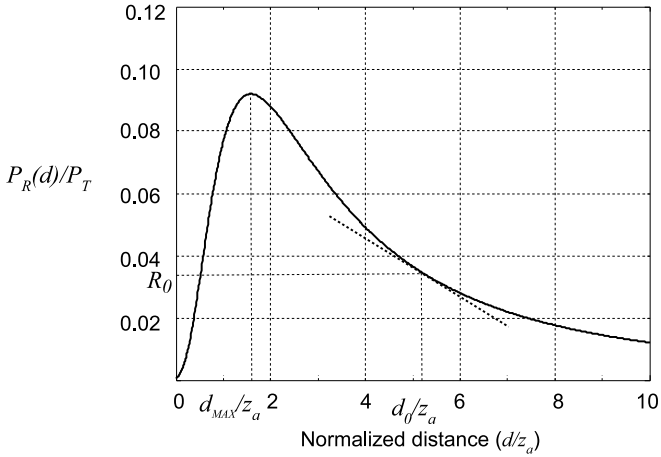


Fig. 2. Typical dependence of the power ratio with the normalized distance.

$$v_R(t) = A \cdot v_L(t) \cdot (R_0 + R_1 \cdot s(t)) \quad (6)$$

The coefficients  $R_0$  and  $R_1$  involved in the linear approximation can be analytically evaluated from the optical power (see Eqn. 2) and its first derivative (see Eqn. 10), both computed at the target mean distance  $d_0$ .

If the LED stimulus  $v_L(t)$  is constant, the received signal contains an AC component that represents the vibration  $s(t)$  with a scale factor that depends on the first derivative  $R_1$  of the curve in Fig. 2 and on the coefficient  $A$ . The former can be analytically evaluated provided that the working distance is either known or it can be somehow estimated, for example by adding another receiving fiber to the sensing head. The term  $A$  depends on the chain gains and on the target reflectivity, which, in general, are both not known and furthermore may change with time.

### III. THE REFLECTIVITY COMPENSATION TECHNIQUE

The solution proposed in this paper is rather different from what already presented [5] and it is based on the spectral analysis of the received signal upon sinusoidal modulation of the incident light  $v_L(t) = A_0 + A_L \cdot \sin(\omega_L t)$ ; when the vibration  $s(t) = A_V \cdot \sin(\omega_V t)$  is sinusoidal too, the received signal becomes:

$$\begin{aligned} v_R(t) = & \underbrace{A \cdot A_0 \cdot R_0}_{V_0} + \underbrace{A \cdot A_0 \cdot A_V \cdot R_1 \cdot \sin(\omega_V t)}_{V_1} + \\ & + \underbrace{A \cdot R_0 \cdot A_L \cdot \sin(\omega_L t)}_{V_2} + \\ & + \underbrace{A/2 \cdot R_1 \cdot A_V \cdot A_L \cdot \cos[(\omega_L - \omega_V)t]}_{V_3} + \\ & + \underbrace{A/2 \cdot R_1 \cdot A_V \cdot A_L \cdot \cos[(\omega_L + \omega_V)t]}_{V_4} \quad (7) \end{aligned}$$

In this case the target behaves like a mixer for the optical beams; therefore the received signal has five spectral components, as shown in Fig. 3, each depending on the unknown term  $A$ . Thus to determine the amplitude of the vibration  $A_V$  independently from  $A$ , in principle it is sufficient to consider the ratio of any term containing  $A_V$  with a term not containing  $A_V$ ; however, from a practical point of view and in order to compensate also the amplitude fluctuations of the LED emissions, there are only two possible solutions:

1. The vibration amplitude is obtained as the ratio of the component at the vibration frequency and the DC component. This solution is easier to implement when dealing with low frequency vibrations but it may introduce relevant disturbances since the DC component can be affected by errors due to the ambient light and the offsets and drifts of the electronic circuitry.
2. The vibration amplitude is obtained as the ratio of the component  $V_2$  and the component at the LED signal frequency  $V_3$ . This solution involves only AC components, avoiding the disturbances due to the DC term. Moreover, working with a high LED modulation frequency allows moving the beat signal  $V_3$  (i.e. the component that is proportional to the vibration amplitude) farther away from the disturbances related to the mains signals, thus improving the overall accuracy. In addition, with this approach it is possible to take advantage of the mixing effect when measuring high frequency vibrations and shift down the beat signal at a frequency low enough to be measured also with low performance devices. With some limitations in the vibration bandwidth [7], this technique can be also employed to measure non sinusoidal vibrations converted to low frequencies.

In the case of the technique that involves AC components only, the amplitude of the vibration signal can be obtained by measuring the amplitude of components  $V_3$  and  $V_2$  respectively at the beat frequency  $\omega_L - \omega_V$  and at the LED stimulus frequency  $\omega_L$ . The vibration amplitude can be thus derived from Eqn. 7 as:

$$A_V = \frac{V_3}{V_2} \cdot \frac{2|R_0|}{R_1} \quad (8)$$

The ratio between the spectral components compensates for possible time variations of the target reflectivity or the amplifier gains, while the ratio  $\frac{|R_0|}{R_1}$  acts as a scale factor that can be analytically computed from the fiber characteristics and the target distance using Eqn.s 2 and 10 obtained from the theoretical model:

$$\frac{|R_0|}{R_1} = R_{01}(d_0) = \frac{\zeta(d_0)^3}{16 - 2\zeta(d_0)^2} \frac{z_a}{2} \quad (9)$$

Relying on the theoretical model to compute the scale factor it is possible to measure the vibration amplitude without the need of calibrations. However, in the presence of a diffusive target like in the test-set described in

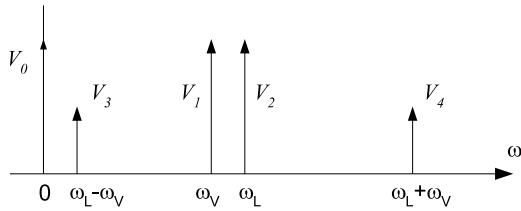


Fig. 3. Representation of the spectral components of the detected signal upon sinusoidal light modulation.

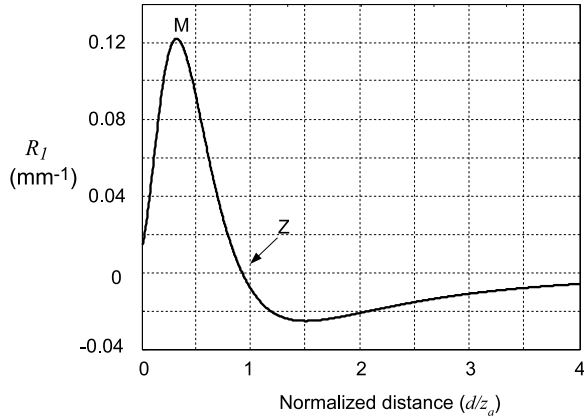


Fig. 4. Sensitivity as a function of the target normalized distance.

the experimental results, the optical behavior of the sensing systems can be significantly different from the model of Eqn. 2. In these cases, a better performance can be achieved only taking into account the real optical behavior of the sensing systems.

#### IV. SENSITIVITY AND UNCERTAINTY ANALYSIS

The value of the fiber-to-target distance  $d_0$  strongly affects the sensor behavior, since it influences both the sensitivity and metrological performance.

The sensitivity is directly proportional to the terms included in  $V_3$ , namely  $A$ ,  $R_1$ , and  $V_L$ . Therefore, the sensitivity can be improved increasing the values of  $A$  and  $V_L$  when possible (i.e. using a high reflectivity target and a high LED driving current), and maximizing  $R_1$  that is the first derivative of the optical power and is dependent on the distance  $d$  as:

$$R_1(d) = \frac{\partial P_r/P_t}{\partial d} = R_0 \cdot \left( \frac{16}{\zeta^3} - \frac{2}{\zeta} \right) \cdot \frac{2}{z_a} \quad (10)$$

A typical behavior of  $R_1$  with distance is shown in Fig. 4 considering the same POF used in Sect. II.

The sensitivity is maximum for a normalized distance of about  $d/z_a = 0.3165$  (point M) and is zero (point Z) when the optical power is maximum, that is for  $d = d_{MAX}$ .

However, in this application where the target distance must be known in order to measure the vibration amplitude using (8), it is also important to minimize the uncer-

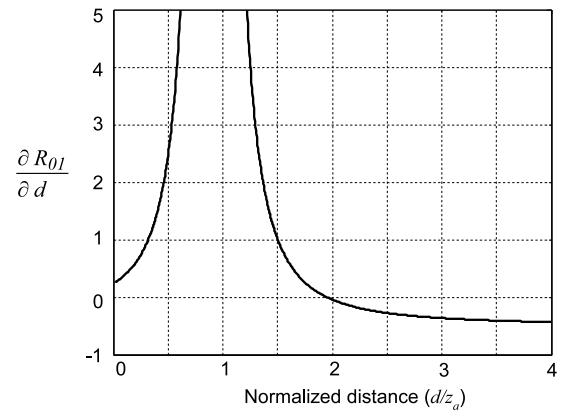


Fig. 5. Sensitivity of the scale factor with the target distance.

tainty of the scale factor  $R_{01}$ . This uncertainty depends on the target distance  $d_0$ , on  $z_a$  and on the model uncertainty that is due to deviations of the physical behavior from the theoretical model described with (2). The latter accounts for several factors like the non uniform reflectivity of the surface, the uncontrolled angle between the fiber tips and the target, the roughness of the fiber tips, etc. Since some of these terms depend on the specific sensor arrangement, a quantitative evaluation will be provided empirically (see Sect. V,B).

The effect of the distance  $d_0$  on  $R_{01}$  can be obtained using the common uncertainty propagation rules [8]. The sensitivity of  $R_{01}$  with the target distance  $d$  can be therefore expressed analytically as:

$$\frac{\partial R_{01}}{\partial d} = \frac{48\zeta^2 - 2\zeta^4}{(16 - 2\zeta^2)^2} \quad (11)$$

The  $R_{01}$  sensitivity behavior is shown in Fig. 5 where is possible to notice that the highest sensitivity is for small target distances, while for a normalized distance of about  $d/z_a \cong 2$  the sensitivity is zero. This means that around this point the scale factor uncertainty does not depend - at least to a first approximation - on the uncertainty of the distance  $d_0$ , which can be therefore known in an approximate way.

However, the scale factor  $R_{01}$  depends also on  $z_a$ , which is related to the fiber geometrical and optical characteristics, and that can be either computed or measured using (3). Fig.6 shows the relative extended uncertainty ( $k = 2$ ) of the scale factor when  $z_a = 1.75$  mm and when both the standard uncertainties of  $d_0$  and  $z_a$  are equal to 0.1 mm.

It is evident from Fig.6 that, to reduce the uncertainty due to the scale factor, one should work at large distances, although in this range the signals are small, thus increasing the uncertainty due to the measurement of the spectral components in (8). In other words, the sensor working position has to be chosen as a compromise between the sensitivity and the uncertainty, both highest for short distances.

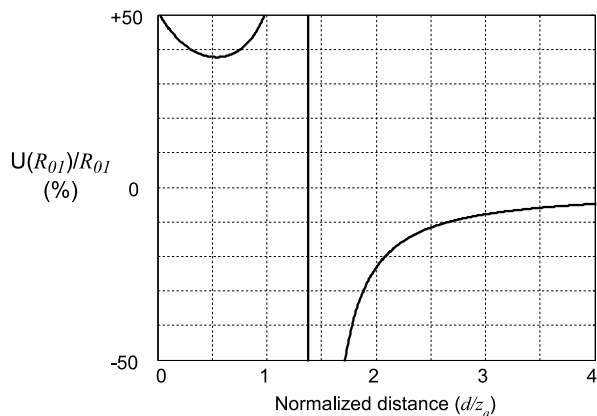


Fig. 6. Extended relative uncertainty of the scale factor  $R_{01}$ .

## V. EXPERIMENTAL RESULTS

Different types of tests were carried out with a twofold objective: assess the performances of the proposed system comparing the readings with those obtained from other devices or technologies, and evaluate its applicability in conditions of practical relevance from the point of view of perspective applications. These tests include:

- the verification of the reflectivity compensation technique using a vibrating target having the surface of different colors and kept at a constant distance from the sensing head;
- the comparison of the readings with those achievable from a commercial calibrated accelerometer under constant reflectivity but varying target distance conditions;
- the determination of the resolution using as a reference a precision computer controlled micro-positioning device;
- the assessment of the high frequency measurement capabilities using a piezoelectric ultrasonic transducer driven at about 40 kHz.

The last two tests have been already described in [9], while the others have been extended or added in this paper and are therefore presented in detail in the following.

The sensing system arranged to carry out the tests was composed of a 670 nm LED and of a photodiode both having a bandwidth of 10 MHz and equipped with standard SMA connectors for POF. About 2 m of PMMA POF with a core diameter of 0.98 mm were employed to carry out the LED light to and from the target. The LED driver and the PD amplifier are custom made circuits designed to have suitable gains and a bandwidth greater than 1 MHz. Commercial signal generators were employed to generate the drive the LED and the vibration actuator. The detected signal was acquired using a digital acquisition board having 16 bit of resolution. The acquired signals were thus processed using an FFT algorithm in order to extract the spectral components amplitudes.

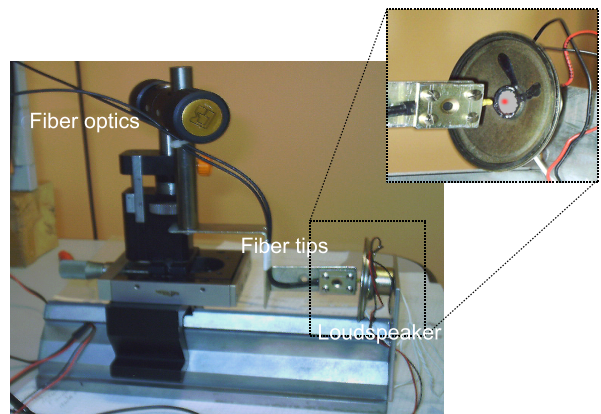


Fig. 7. Photograph of the test-set based on a loudspeaker used to assess the reflectivity compensation technique.

### A. Reflectivity compensation

In order to verify the effectiveness of the proposed compensation technique, tests were carried out employing a small loudspeaker as a vibrating target. A tiny piece of paper was glued in the middle of the moving coil and then painted with various colors so that the reflected optical power from the least reflecting paper was five times smaller than that measured in the case of the most reflecting one (white color).

The LED and the loudspeaker were driven with sinusoidal stimuli at 600 Hz and at 370 Hz, respectively. The received signal was amplified and then acquired by means of an acquisition board whose sampling rate was set to 10 kHz. The acquired signal was processed in order to measure the amplitudes of the components  $V_2$  at 600 Hz and  $V_3$  at 230 Hz. Fig. 7 shows a detail of the arranged test set. The fiber tips were kept at a distance  $d_0 = 5$  mm from the target, a value that represents a good compromise between sensitivity, high for small distances, and uncertainty, which reduces increasing the distance, according to the discussion in Sect. IV.

The speaker was driven at increasing current intensities to have different vibration amplitudes. Fig. 8 shows the measured amplitude of component  $V_3$  for four different values of the surface reflectivity corresponding to white, yellow, light blue and dark gray colors, respectively. As it is clearly evident, the amplitude of this spectral component is proportional to the vibration amplitude but is also strongly dependent on the surface reflectivity, as expected.

The vibration amplitude obtained applying (8) to the components  $V_3$  and  $V_2$  is shown in Fig. 9, where it is possible to note that the curves show an excellent overlap that is limited only by factors such as the system reproducibility and the working distance uncertainty.

### B. Comparison tests with a commercial accelerometer

Comparative tests with a calibrated piezoelectric accelerometer were also performed to evaluate the response of the proposed sensor at constant target reflectivity but varying working distance conditions. An electrodynamic

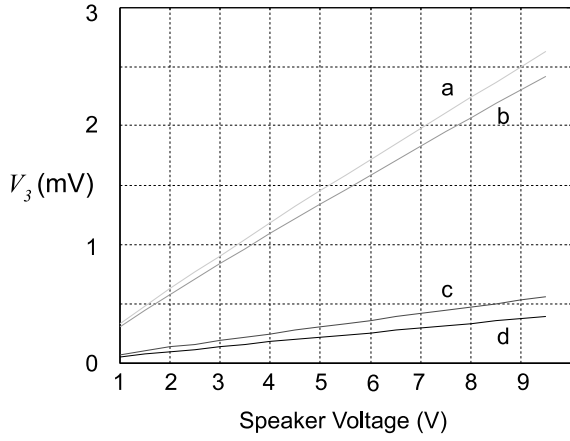


Fig. 8. Measured  $V_3$  component amplitude for different values of reflectivity of the loudspeaker surface.

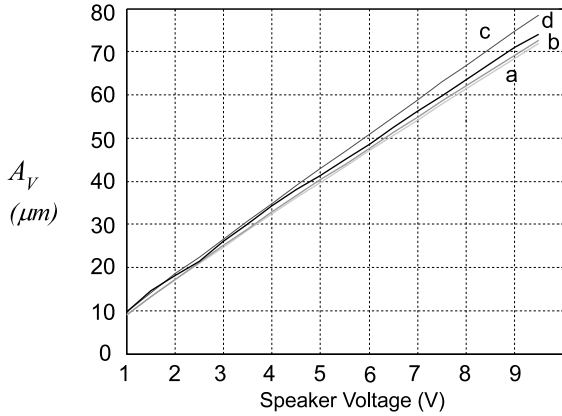


Fig. 9. Ratio amplitude between components  $V_3$  and  $V_2$  for different value of reflectivity of the loudspeaker surface.

shaker was employed in this case to generate a steady sinusoidal vibration at  $f_V=1473$  Hz (see Fig. 10). The fiber tips were placed in front of the shaker fixture as close as possible to the reference accelerometer. The LED modulation frequency was set to 10 kHz and therefore the beat component related to the vibration signal was at 8527 Hz. The choice of a high LED modulation frequency is useful to reduce aliasing phenomena in presence of distorted vibration signals and it also avoids the interference of spurious optical signals due, for example, to fluorescent lights. The accelerometer output was acquired and the spectral component at the vibration frequency extracted; then the vibration amplitude was obtained as  $A_V^{acc} = a/(2\pi f_V)^2$ , being  $a$  the peak value of the acceleration. The recovered peak of the vibration amplitude was  $A_V^{acc} = 3.2 \mu\text{m}$  with a standard uncertainty of about 5% mainly due to the accelerometer frequency response.

The distance  $z_a$  was evaluated from the optical power curve, obtaining  $z_a = 1.75$  mm with a standard uncertainty of about 0.1 mm. Then, this value was employed to derive the scale factor  $R_{01}$  from (9).

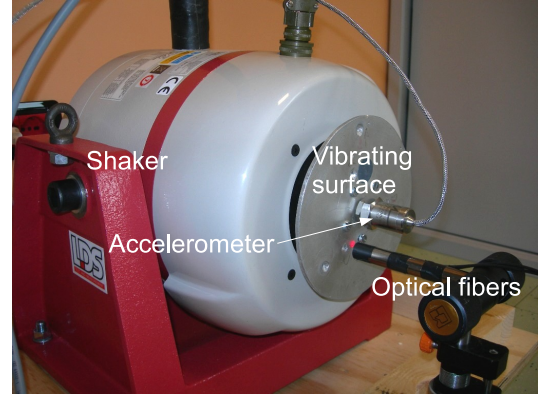


Fig. 10. Photograph of the test-set based on an electrodynamic shaker used in the comparisons with the calibrated accelerometer.

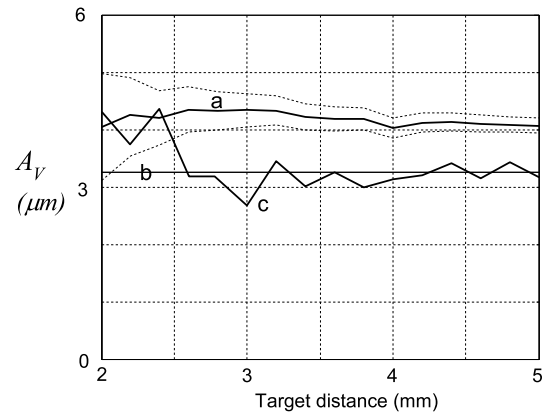


Fig. 11. Vibration amplitude measured at different target distances: a) POF sensor with scale factor computed from the theoretical model of the optical link; b) amplitude obtained processing the accelerometer output c) POF sensor with scale factor empirically evaluated.

The result of the comparisons are reported in Fig. 11; the readings from the proposed sensor (curve a, together with its uncertainty band obtained with a coverage factor  $k = 2$ ) show that the measured vibration amplitude is almost independent from the distance. However, it is possible to note a relevant difference between this curve and that obtained from the accelerometer (curve b, without the uncertainty band for clarity of the picture). This can be ascribed to the theoretical model used to compute the scale factor  $R_{01}$ . Actually, this difference is reduced using the empirical scale factor computed measuring the optical power  $R_0$  and its first derivative  $R_1$ . Curve c shows the vibration amplitude still obtained using Eqn. 8 but using the empirical scale factor. In this application the error due to the simplifications intrinsic in the theoretical model is thus not negligible with respect to the distance uncertainty. Anyway, it is important to highlight that curve a) is compensated both for the reflectivity of the target surface and for the gains of the measurement chain even if it has been obtained without any calibration of the sensor. On the other hand, curve c) requires a calibration to be carried


out after that the optical sensor has been arranged.

## VI. CONCLUSIONS

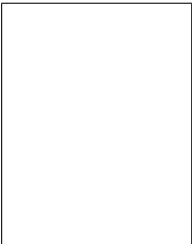
An innovative and low cost measurement system to measure vibrations using a non-contact approach, independent from the vibrating surface reflectivity has been proposed and experimentally evaluated. The system uses plastic optical fibers for the realization of the sensing head and a simple spectral analysis to evaluate the amplitude of the vibrations, compensating for the target reflectivity and offsets and gains in the measurement chain. A number of experiments to assess the performance of the developed system have been carried out using vibrating surfaces with different values of reflectivity and frequency ranging from few hertz to several tens of kilohertz. Comparisons with other techniques or reference systems have shown the capability of the system to measure vibration amplitudes below  $1\ \mu\text{m}$  up to about 40 kHz.

## REFERENCES

- [1] P.M.B.S. Girao, O.A. Postolache, J. Faria, J.M.C.D. Pereira, "An overview and a contribution to the optical measurement of linear displacement", *IEEE Sensors Journal*, v. 1, n. 4, pp. 322-331, 2001.
- [2] S. Donati, "Electro-optical instrumentation: sensing and measuring with lasers", *Upper Saddle River: Prentice Hall*, 2004.
- [3] P. Castellini, M. Martarelli, E.P. Tomasini, "Laser Doppler vibrometry: development of advanced solutions answering to technology's needs", *Mechanical System and Signal Processing*, v. 20, pp. 1265-1285, 2006.
- [4] J.B. Faria, "A Theoretical Analysis of the Bifurcated Fibre Bundle Displacement Sensor", *IEEE Transactions on Instrumentation and Measurement*, vol. 47, no. 3, pp. 742-747, 1998.
- [5] R. Dib, Y. Alayli, P. Wagstaff, "A broadband amplitude-modulated fibre optic vibrometer with nanometric accuracy", *Measurement, Elsevier Science*, vol. 35, no. 2, pp. 211-219, 2004.
- [6] X. Li, K. Nakamura, S. Ueha, "Reflectivity and illuminating power compensation for optical fibre vibrometer", *Meas. Sci. Technol.*, vol. 15, pp. 1773-1778, 2004.
- [7] L. Schnell (ed.), "Technology of Electrical Measurements", *Chichester: John Wiley and Sons*, 1993.
- [8] ISO, "Guide to the Expression of Uncertainty in Measurement", October 1993.
- [9] A. Buffa, G. Perrone, A. Vallan, "A Plastic Optical Fiber Sensor for Vibration Measurements", *IEEE International Instrumentation and Measurement Technology Conference Proceeding, 2008, I2MTC 08, Vancouver, Canada, 12-15 May, 2008*.



**Alberto Vallan** was born in Italy in 1967. He received the M.S. degree in Electronic Engineering in 1996 from Politecnico di Torino, Italy, and in 2000 the Ph.D. degree in Electronic Instrumentation from the University of Brescia, Italy. He is currently assistant professor with the Electronic Department of Politecnico di Torino. His main research interests are digital signal processing and development and characterization of sensors and instruments for industrial applications.



**Guido Perrone** was born in Italy in 1965. He holds a Ph.D. in Electromagnetics from Politecnico di Torino (Italy), where he is currently assistant professor, lecturing on Optical Components and Fibers and on Microwave Devices. His research activity is mainly in the fields of fiber optical sensors and of high power fiber lasers. Dr. Perrone is member of IEEE/MTTS, of IEEE/LEOS and of the Optical Society of America.